Plume-induced stress in pulsed-laser deposited CeO_2 films

D. P. Norton,[a] C. Park, J. D. Budai, S. J. Pennycook, and C. Prouteau[b]
Oak Ridge National Laboratory, Solid State Division, Oak Ridge, Tennessee 37831-6056

(Received 1 October 1998; accepted for publication 16 February 1999)

Residual compressive stress due to plume-induced energetic particle bombardment in CeO_2 films deposited by pulsed-laser deposition is reported. For laser ablation film growth in low pressures, stresses as high as 2 GPa were observed as determined by substrate curvature and four-circle x-ray diffraction. The amount of stress in the films could be manipulated by controlling the kinetic energies of the ablated species in the plume through gas-phase collisions with an inert background gas. The film stress decreased to near zero for argon background pressures greater than 50 mTorr. At these higher background pressures, the formation of nanoparticles in the deposited film was observed. © *1999 American Institute of Physics.* [S0003-6951(99)04215-1]

Understanding and controlling stresses in thin films is an important issue for any deposition processes. Stress can lead to film cracking and delamination, as well as to variations in film properties. Stresses due to thermal expansion coefficient mismatch or lattice mismatch between the film and substrate are generally independent of the deposition process. However, specific defect structures inherent to the deposition process can introduce additional compressive or tensile stress components.[1] Metal films, such as Cu, are often characterized by tensile strain when deposited by evaporation.[2] The origin of this tensile strain is generally believed to be an attractive interaction across voids within the film.[1] In contrast, the simultaneous bombardment with energetic ionic or neutral species during film deposition can result in compressive stress for many systems.[3] For example, intrinsic compressive stress has been observed in Y_2O_3 films deposited by reactive sputtering due to the bombardment of energetic Ar ions during deposition.[4] The origin of compressive stress due to energetic bombardment is associated with subsurface damage from the impinging energetic species leading to interstitial defects. The kinetic energy necessary for the onset of recoil implantation of surface atoms into the film interior through bombardment is material dependent, but is often observed for ion bombarding energies of a few eV or greater.[5]

For many thin-film systems, the tailoring of stress in the film becomes possible through the bombardment of the depositing film with energetic species during film growth. In pulsed-laser deposition (PLD), the kinetic energies of ions and neutral species in the ablation plume can range from a few tenths to as high as several hundred eV. These energies should be sufficient to modify the stress state of films through defect formation, as has been documented for ion-beam-assisted approaches. Unfortunately, few studies have addressed this issue for PLD. One study on the homoepitaxial growth of $SrTiO_3$ using PLD showed the presence of compressive stress in the films as indicated by lattice distortion.[6] Further work is needed to better understand the role of ablation energies in determining film stress, in particular, to delineate the effects of plume kinetic energies from other possible sources of lattice distortion, including deviations in oxygen content in the films.

We have examined the intrinsic stress induced by energetic species in the laser ablation plume for CeO_2 films deposited using pulsed-laser deposition. Cerium oxide is an interesting oxide buffer layer due to a favorable lattice match with silicon and the high-temperature superconducting materials, and is an important material for optical coatings due to its relatively high refractive index.[7–13] In addition, CeO_2 is an attractive binary oxide model system, since it has been the subject of previous studies on ion bombardment effects during film growth.[14,15] In this study, we have attempted to delineate the specific effects of plume energetics in determining the compressive stress by manipulation of the ion and neutral kinetic energies using inert Ar as the background gas. Previous work indicates that the ablation of CeO_2 results in a significant flux of ejected Ce^+ ions with kinetic energies ranging from 10 to 50 eV for laser energy densities on the order of 1.7–6.7 J/cm^2 in a background pressure of 10^{-6} Torr or less.[16] At higher background pressures, gas-phase collisions between the ablated species and background gas molecules reduce the kinetic energies, allowing one to tune the energy distribution.[17] The specific energies depend on the ablation process at the target and the collision cross section of the ablated species with the background gases. The oxidation kinetics are kept relatively unchanged by maintaining a fixed oxygen partial pressure for different Ar background pressures.

A KrF (248 nm) excimer laser was used as the laser ablation source. The laser energy density was maintained at ~3 J/cm^2 with a repetition rate of 5 Hz. Deposition was performed at 100 and 700 °C in order to delineate the effects of thermal expansion mismatch and *in situ* annealing at the deposition temperature. The substrates used were (100) YSZ and thin (111) Si. The (111) Si substrates were useful for determining stress by measuring the degree of bowing induced in the substrate due to the stress in the (111)-textured polycrystalline CeO_2 films. The films on the (100) YSZ were generally epitaxial for both the 100 and 700 °C deposition temperatures. These films were used to measure the stress-induced lattice parameter distortion. The thermal expansion

[a]Electronic mail: ntn@ornl.gov
[b]Also with the Dept. of Physics, University of Illinois at Chicago, Chicago, IL 60607-7059.

 © 1999 American Institute of Physics
Downloaded 12 Mar 2002 to 128.219.47.178. Redistribution subject to AIP license or copyright, see http://ojps.aip.org/aplo/aplcr.jsp

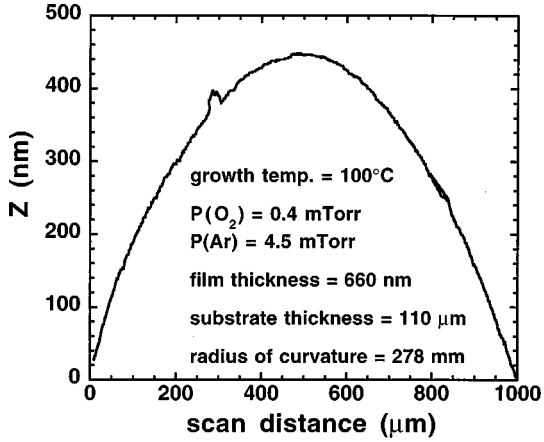

FIG. 1. Surface profile scan of CeO_2 film deposited on thin Si(111).

coefficient of YSZ is nearly identical to that for CeO_2. Base pressure for the vacuum system was $\sim 5\times10^{-6}$ Torr. The total background pressure was varied from 5×10^{-6} to 2×10^{-1} Torr using argon and oxygen as the background gases. For total pressure greater than or equal to 4×10^{-4} Torr, the oxygen partial pressure was maintained near 4×10^{-4} Torr. With the beam scanning setup used in these experiments, thickness uniformity was on the order of $\pm5\%$ or better.

For CeO_2 films deposited at 100 °C using PLD, we observe significant compressive stress for films deposited at lower total background pressures due to energetic ions and neutral species in the ablation plume. Figure 1 shows a surface profile scan of a 660 nm thick CeO_2 film deposited at 5 mTorr background pressure and 4×10^{-4} Torr oxygen partial pressure on 110 μm thick Si showing significant bowing due to the compressive stress in the film. Based on the mechanical properties of the Si substrate, one can calculate the stress in the film evident in the substrate bowing using the expression

$$\sigma_s = E_s d^2[6(1-\nu_s)tR]^{-1},$$

where ν_s is Poisson's ratio of the substrate, E_s is the Young's modulus of the substrate, t is the film thickness, d is the substrate thickness, and R is the radius of curvature for the Si substrate. Using this, a compressive stress of 2 GPa is calculated for this sample.

The presence of compressive strain was also manifested by a tetragonal distortion of the CeO_2 crystal lattice for epitaxial films on (100) YSZ. Figure 2(a) shows the c-axis lattice parameter of epitaxial CeO_2 films deposited on (100) YSZ substrates for various background pressures ranging from 10^{-5} to 200 mTorr. The oxygen partial pressure is maintained at 4×10^{-4} Torr for all cases except for the lowest pressure in which no background gas was intentionally introduced. The large lattice distortion is a manifestation of both the stresses in the film as well as defects in the film, such as oxygen vacancies, that expand the CeO_2 unit cell volume independent of stress. In order to delineate these effects, we must determine the ''unstrained'' lattice spacing that the film would assume given a release of the stress. From measurements of both the in-plane and out-of-plane

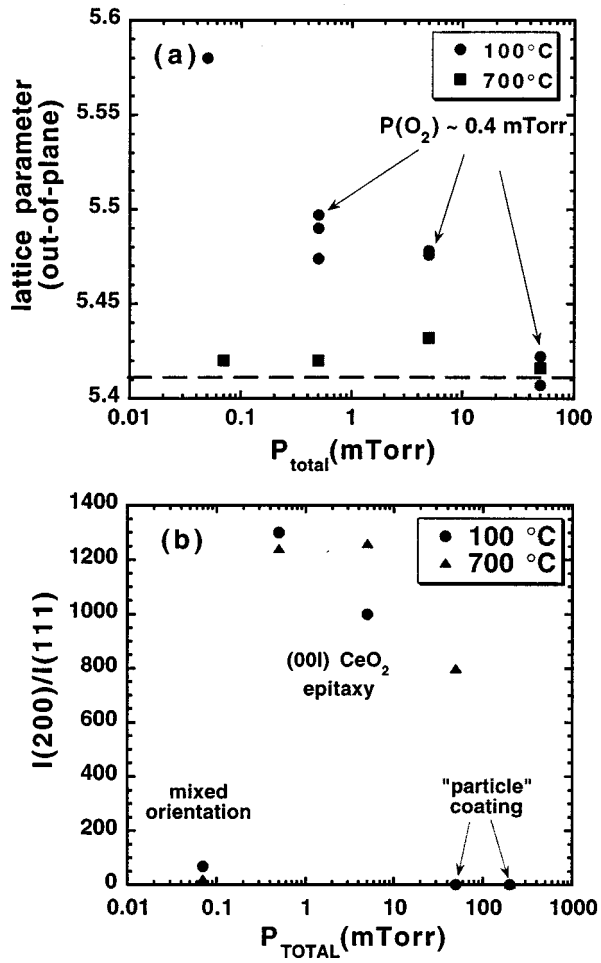

FIG. 2. Plot of (a) out-of-plane lattice parameter and (b) x-ray diffraction $I(200)/I(111)$ intensity ratio as a function of total background pressure for CeO_2 films deposited using PLD.

lattice spacing of the film, the nominally cubic lattice parameter of the film in the absence of stress can be determined[6] by the equation

$$a_0 = [(1-\nu_f)a_\perp + 2\nu_f a_\parallel][1-\nu_f]^{-1},$$

where ν_f is the Poisson's ratio of CeO_2, $a_\perp$ is the out-of-plane lattice parameter, and $a_\parallel$ is the in-plane lattice parameter of the film. From this, one can determine the film stress σ_s using

$$\sigma_s = [E_f(a_\perp - a_0)][(1-\nu_f)a_0]^{-1},$$

where E_f is the Young's modulus, $a_\parallel$ is the film in-plane lattice parameter, and a_0 is the ''unstrained'' lattice parameter of the CeO_2 film. Table I shows the compressive stress as a function of total background pressure for several films.

TABLE I. Lattice spacing and strain for various CeO_2 films.

Temp. (°C)	$P(O_2)$ (mTorr)	P(Total) (mTorr)	$a_\perp$ (Å)	$a_\parallel$ (Å)	a_0 (Å)	σ_{XRD} (GPa)	σ_{Bowing} (GPa)
100	0	0.05	⩾5.5	5.5	5.5	⋯	0.8
100	0.4	0.4	5.477	5.403	5.443	1.7	⋯
100	0.4	0.4	5.487	5.40	5.45	2.0	2.9
100	0.4	5	5.482	5.42	5.454	1.5	2.0
100	0.4	50	5.4	⋯	⋯	⋯	⋯
700	0.4	0.4	5.417	5.41	5.414	0.17	⋯

Downloaded 12 Mar 2002 to 128.219.47.178. Redistribution subject to AIP license or copyright, see http://ojps.aip.org/aplo/aplcr.jsp

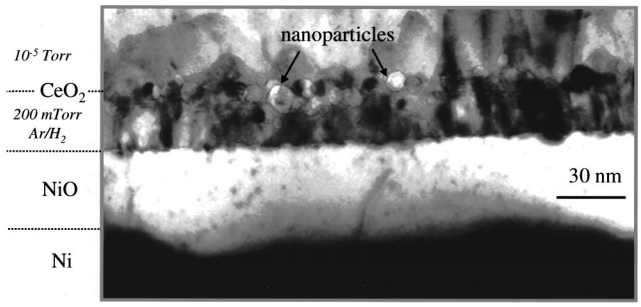

FIG. 3. Cross-section transmission electron microscope image of CeO_2 film deposited on (100) Ni showing the presence of nanoparticles.

For films deposited at constant oxygen pressure, the compressive stress decreases as the background gas pressure is increased, reflecting a reduction in the kinetic energy of ablated species through collisions. The relatively low stress in films deposited in vacuum probably reflects the poor crystallinity due to oxygen deficiency. Also shown in Table I is the ''unstrained'' lattice spacing a_0, as a function of total background pressure. For films deposited at 5 mTorr or less, the unstrained lattice parameter is significantly expanded relative to the bulk CeO_2 value. This suggests that the energetic Ce^+ ions preferentially sputter oxygen atoms, leaving an oxygen-depleted CeO_2 lattice. This is consistent with Monte Carlo simulations that show a lower-energy threshold for the removal of oxygen off of the CeO_2 surface as compared to Ce.[14] A volume expansion is typical for oxygen deficiency in bulk CeO_{2-x}. The largest unstrained lattice expansion is observed for the film deposited in vacuum. A preliminary measurement of the kinetic-energy distribution for the ablation plume in vacuum was performed using an ion probe. Energies of several hundred eV were observed. These energies are relatively high for laser ablation plumes, and account for the significant lattice distortions in the films.

For films deposited at 700 °C, the stress and volume expansion in the films was significantly less than that observed at 100 °C, although it was not zero. The reduction in stress and lattice distortion is presumably due to the *in situ* annealing of plume-induced defects. The observation of some stress and lattice distortion reiterates the general need to consider plume-induced stress even in high-temperature film growth using PLD.

In addition to the stress, it is instructive to also consider the crystallinity of the films as monitored by x-ray diffraction (XRD) peak intensity. Figure 2(b) shows the (200)/(111) peak intensity ratio for the epitaxial CeO_2 films on (100) YSZ. Superior epitaxial crystallinity is achieved for the intermediate pressure range 0.5–5 mTorr. At the higher pressures, the degree of epitaxy diminishes drastically. In fact, the films deposited in 50 and 200 mTorr at 100 °C resemble a particulate film with no adhesion to the substrate. It is unclear whether these particles nucleate in the gas or on the substrate surface. Figure 3 shows a cross-section transmission electron microscopy image of a CeO_2 film grown epitaxially on a (001) Ni surface at a deposition temperature of 710 °C. The initial 30 nm was nucleated in the presence of the 200 mTorr Ar/2% H_2 mixture. This was followed by deposition in vacuum (10^{-5} Torr base pressure) and 4×10^{-4} Torr oxygen background. A transition in film microstructure is observed for the different background pressures. The film deposited at 200 mTorr Ar/2% H_2 exhibits a uniaxial structure while the microstructure of the film grown at 10^{-5} Torr vacuum is reminiscent of a columnar structure. These changes in microstructure are similar to that observed for films deposited in the presence of an energetic ion beam. Note also that the initial layer deposited at high background pressure is decorated with nanocrystals. The size of these nanoparticles ranges from 5 to 10 nm in diameter. The layers deposited at lower pressures have no nanoparticles. This is consistent with the particulate-like coatings for the CeO_2 films deposited at 100 °C in high background pressure, and reiterates the fact that the formation of nanoparticles by laser ablation must be considered in film growth at background pressures greater than 50 mTorr. This will be particularly true for binary oxide films where the formation of stable nanoparticle phases involves only two atomic constituents.

In conclusion, we have shown that energetic ions and/or neutral species in a laser ablation plume can induce significant compressive stress in deposited films. To some extent, the background pressure during ablation can be used to manipulate the ion energies and control the resulting compressive stresses. However, a sufficient increase in the background pressures may lead to the formation of nanoparticles in the deposited films.

This research was sponsored by the Oak Ridge National Laboratory, managed by the Lockheed Martin Energy Research Corp., for the U.S. Department of Energy, under Contract No. DE-AC05-96OR22464.

[1] E. S. Machlin, *Materials Science in Microelectronics* (GIRO, 1995), pp. 157–184.
[2] R. A. Roy, J. J. Cuomo, and D. S. Yee, J. Vac. Sci. Technol. A **6**, 1621 (1988).
[3] R. A. Roy and D. S. Yee, in *Handbook of Ion Beam Processing Technology*, edited by J. J. Cuomo, S. M. Rossnagel, and H. R. Kaufman (Noyes, NJ, 1989), pp. 194–218.
[4] H. M. Choi and S. K. Choi, J. Vac. Sci. Technol. A **13**, 2832 (1995).
[5] K.-H. Muller, in Handbook of Ion Beam Processing Technology, edited by J. J. Cuomo, S. M. Rossnagel, and H. R. Kaufman (Noyes, NJ, 1989), pp. 241–278.
[6] E. J. Tarsa, E. A. Hachfeld, F. T. Quinlan, J. S. Speck, and M. Eddy, Appl. Phys. Lett. **68**, 490 (1996).
[7] T. Chikyow, S. M. Bedair, L. Tye, and N. A. El-Masry, Appl. Phys. Lett. **65**, 1030 (1994).
[8] M. Yoshimoto, K. Shimozono, T. Maeda, T. Ohnishi, M. Kumagai, T. Chikyow, O. Ishiyama, M. Shinohara, and H. Koinuma, Jpn. J. Appl. Phys., Part 2 **34**, L688 (1995).
[9] C. Tian, Y. Du, and S.-W. Chan, J. Vac. Sci. Technol. A **15**, 85 (1997).
[10] R. L. Goettler, J. P. Maria, and D. G. Schlom, Mater. Res. Soc. Symp. Proc. **474**, 333 (1997).
[11] D. P. Norton, C. Park, B. Saffian, J. D. Budai, A. Goyal, D. K. Christen, D. M. Kroeger, D. Lee, Q. He, and M. Paranthaman, Mater. Res. Soc. Symp. Proc. **474**, 401 (1997).
[12] M. W. Denhoff, B. F. Mason, H. T. Tran, and P. D. Grant, Mater. Res. Soc. Symp. Proc. **401**, 339 (1996).
[13] X. D. Wu, R. C. Dye, R. E. Muenchausen, S. R. Foltyn, M. Maley, A. D. Rollett, A. R. Garcia, and N. S. Nogar, Appl. Phys. Lett. **58**, 2165 (1991).
[14] K.-H. Muller, Appl. Phys. A: Solids Surf. **40**, 209 (1986).
[15] M. S. Al-Robaee, K. Narasimha Rao, and S. Mohan, J. Appl. Phys. **71**, 2380 (1992).
[16] L. G. Coccia, G. C. Tyrrell, J. A. Kilner, D. Waller, R. J. Chater, and I. W. Boyd, Appl. Surf. Sci. **96-98**, 795 (1996).
[17] D. B. Geohegan, in *Laser Ablation: Mechanisms and Applications*, edited by J. C. Miller and R. F. Hagland, Jr. (Springer, Berlin, 1991), pp. 28–37.

Downloaded 12 Mar 2002 to 128.219.47.178. Redistribution subject to AIP license or copyright, see http://ojps.aip.org/aplo/aplcr.jsp